PHYSICAL REVIEW E, VOLUME 65, 050601(R)

Liquid-solid transition in a model hard sphere system of block copolymer micelles

V. Castelletto, C. Caillet, and I. W. Hamley*
Department of Chemistry, University of Leeds, Leeds LS2 9JT, United Kingdom

Z. Yang
Department of Chemistry, University of Manchester, Manchester M13 9PL, United Kingdom

(Received 5 September 2001; published 13 May 2002)

The transition between micellar liquid and face-centered-cubic crystalline solid in a solution of an amphiphilic diblock copolymer is investigated by small-angle x-ray scattering and rheology. The system is well described by the hard sphere model and there is no evidence for percolation driven by attractive interactions, in contrast to previous reports. Instead, a coexistence region separates liquid and crystal phases.

DOI: 10.1103/PhysRevE.65.050601 PACS number(s): 83.80.Uv, 82.70.Uv, 82.70.Dd

The fluid-solid transition in soft materials has attracted immense interest due to its importance in technological applications and because it can be studied in model systems experimentally and theoretically. The ''zeroth order'' model for this transition is that for the crystallization of hard spheres, which interact through a purely repulsive potential. Over thirty years ago, computer simulations located the volume fractions at which crystallization and melting occur [1]. Later experimental observations on sterically stabilized colloidal sols confirmed these predictions [2].

Spherical micelles formed by a block copolymer in a selective solvent can be viewed as model colloidal particles. The effective interaction potential between the micelles can be varied by changing the composition and/or molecular weight of the copolymer and thus the size of a micelle and the relative size of the micellar core and corona. If the volume fraction of micelles is sufficiently high, crystallization can occur when the micelles pack into a regular array [3–6]. This corresponds to the formation of a soft solid, sometimes termed ''hard gel'' (based on the existence of a finite yield stress, and a dynamic elastic modulus $G' > 10^4$ Pa [7]). Differences in the effective intermicellar potential lead to the possibility of ordering in body-centered cubic (bcc) or face-centered-cubic (fcc) structures [5,8]. Micelles that act as hard spheres pack into face-centered cubic arrays whereas softer interaction potentials favor a bcc structure. These structures can both be obtained for a purely repulsive potential [9–11]. Attractive interactions will also influence the liquid-solid transition. It has been suggested that when strong attractive interactions are present this transition occurs via percolation, i.e., aggregation of copolymer micelles into an increasingly ramified fractal structure [12–14]. It should be noted that we do not favor the terminology ''gel'' used in the literature for these structures. A polymer gel is a network, however, as used in the context of block copolymer solutions there does not have to be any interpenetration of chains on micelles. The gel is simply a solid structure that results from the packing of micelles. Thus, in the following we refer to ''solid'' and ''soft solid'' rather than ''hard'' and ''soft'' gel [15].

Here we investigate the phase diagram and flow behavior of a solution of block copolymer micelles. A soft solid phase is identified between micellar liquid and solid (crystal) phases. The structure of this soft solid phase has been the subject of recent controversy—it has been suggested that soft solids observed in block copolymer solutions result from aggregation of spherical micelles via percolation into fractal structures [12–14], or that they correspond to highly defective solids [16]. Here, we show that the structure of the soft solid phase formed by a poly(oxyethylene)-poly(oxybutylene) diblock copolymer in water can be described by the hard sphere model. Modeling of small-angle x-ray scattering (SAXS) curves suggests that gelation does not occur through a percolation transition in this system. This is supported by evidence from rheology experiments. Instead, the soft solid corresponds to the region where micellar liquid and crystalline gel phases coexist.

We study aqueous solutions of the diblock copolymer $E_{87}B_{18}$, where E denotes hydrophilic poly(oxyethylene), B denotes hydrophobic poly(oxybutylene), and the subscripts are the number of repeats. The copolymer was synthesized via sequential oxyanionic polymerization. The synthesis and characterization of the copolymer are described elsewhere [17]. Rheology experiments were performed using a Bohlin CVO constant stress rheometer. Care was taken to perform measurements in the linear viscoelastic regime, defined in stress sweeps. The structure of the soft solids was probed using small-angle x-ray scattering at the Synchrotron Radiation Source, Daresbury Lab, UK on beamline 2.1. Samples were heated in sealed brass cells with mica windows. Further details are provided elsewhere [17]. The background and transmission corrected intensity is denoted $I_c(q)$.

Solids have a finite yield stress and do not flow under their own weight [12]. Thus the solid region can be mapped out by mobility experiments. Figure 1 shows the phase boundary determined in this way, i.e., by inverting a test tube containing the soft solid. This procedure has previously been shown to give boundaries in good agreement with more precise rheological measurements of the temperature dependence of the isochronal dynamic shear moduli, G' and G'' [12,18]. This was also confirmed for soft solids of $E_{87}B_{18}$.

Rheology was also used to locate the soft solid region shown in Fig. 1. The transition was apparent from disconti-

*Author to whom correspondence should be addressed.

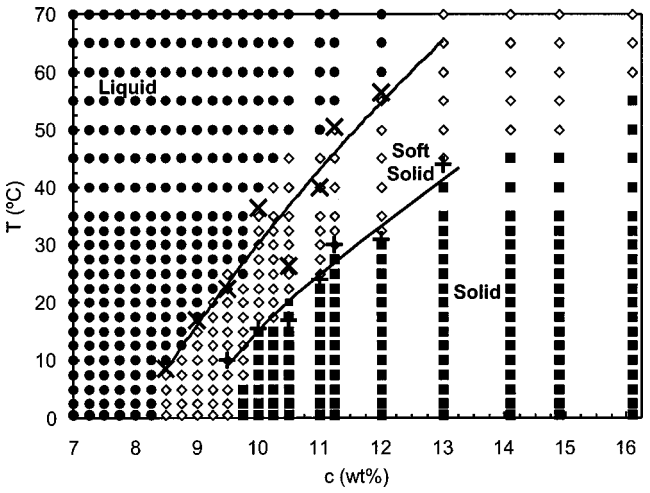

FIG. 1. Phase boundaries for aqueous solutions of block copolymer $E_{87}B_{18}$ determined either by tube inversion (symbols) or rheometry (crosses). The data points are denoted (●) for liquid, (◇) for a soft solid, and (■) for a solid. The rheometry experiments (temperature ramp) provided solid to soft solid transition temperatures (+) and soft solid to liquid transitions (×). The lines are guides to the eye.

nuities in the temperature dependence of G' and G'' in experiments performed at a constant stress and shear frequency. In addition, frequency sweeps were performed at selected temperatures (and at a constant stress) to probe the viscoelastic state of the solution. Data for 9 wt % solutions of $E_{87}B_{18}$ are shown in Fig. 2. At $T=22.5\,°C$, the dynamic moduli

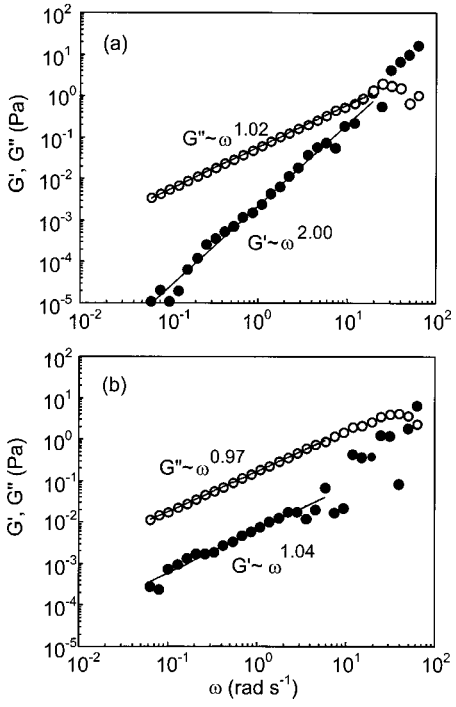

FIG. 2. Frequency dependence of storage modulus G' (●) and loss modulus G'' (○) for 9.0 wt % aqueous solution of block copolymer $E_{87}B_{18}$ at (a) $T=22.5\,°C$ and (b) $T=10\,°C$, with shear stress $\sigma=0.5$ Pa. The lines indicate scaling laws for G' and G''.

exhibit scalings $G'\sim\omega^2$ and $G''\sim\omega^1$ with the frequency ω, characteristic of the terminal response of liquids. However, at 10 °C, G' and G'' obey approximately parallel scaling laws as a function of frequency, as observed for a wide variety of polymer gels [19]. In previous work on a poly(oxyethylene)-poly(oxyproylene)-poly(oxyethylene) triblock ($E_{13}P_{30}E_{13}$) in water, Lobry *et al.* [13] also observed that G' and G'' have identical frequency dependencies ($G'\sim G''\sim\omega^{\Delta}$) close to the transition to a solid. In their case the exponent, Δ, obtained for a soft solid with a concentration $c=10$ wt % was consistent with that calculated [20–22] for a percolating system ($\Delta=0.72$). However, a lower value was obtained for a higher concentration soft solid, which they suggested was related to an increase in the distribution of relaxation times as the packing fraction of micelles increased to approach a glasslike state [13,23]. Although precise measurements of the modulus or viscosity are required to locate the transition between soft solid and micellar liquid or solid phases, remarkably it proved possible to estimate the boundaries of the soft gel just from mobility experiments and these are also shown in Fig. 1. Upon inverting a tube containing a soft solid it was observed that the viscous liquid began to run over a time scale of seconds. This is consistent with the very small, but finite yield stress measured for the soft solid phase (e.g., yield stress $\sigma_y=8$ Pa for a 9 wt % solution at $T=10\,°C$).

Having established the soft solid phase diagram from rheology and tube inversion experiments, SAXS was used to probe changes in the gel structure as a function of concentration and temperature. The small angle x-ray scattering intensity $I(q)$ of an isotropic solution of polydisperse spherical particles can be written, in the local monodisperse approximation [24], as

$$I(q)=k\int_D^{\infty}P(q,R_s)S(q,R_{\mathrm{eff}})f(R_s)dR_s\,, \qquad (1)$$

where k is a normalization constant proportional to the number density of particles, R_s is the micellar core radius, and R_{eff} is the effective radius of interaction between the micelles. $P(q,R_s)$ is the monodisperse micellar form factor, $S(q,R_{\mathrm{eff}})$ is the monodisperse intermicellar structure factor, and $f(R_s)$ is the radius distribution function.

To fit the SAXS data we used an expression for $P(q,R_s)$ based on a homogeneous micellar core with attached Gaussian chains [25]. The six parameters related to the micellar structure are the association number N, the radius of gyration of the E chains, R_g, the displacement of the E chains from the core surface, α, the excess electron densities β_x of a block in the core ($x=s$) or in the corona ($x=c$), and the width of the Gaussian distribution used to describe the polydispersity in micellar size. Fixed values $\alpha=0.4$, $\beta_c=0.025$, and $\beta_s=-0.012$ were found to give good fits.

For the structure factor, we used the analytical expression for hard spheres [26] that is expressed as a function of the hard sphere volume fraction of micelles ϕ and the effective sphere radius, R_{eff}. The only parameter in $S(q,R_{\mathrm{eff}})$ varied is ϕ, since the hard sphere micellar radius was fixed to $R_{\mathrm{eff}}=R_s+2R_g$ and therefore calculated from the fitted $P(q,R_s)$.

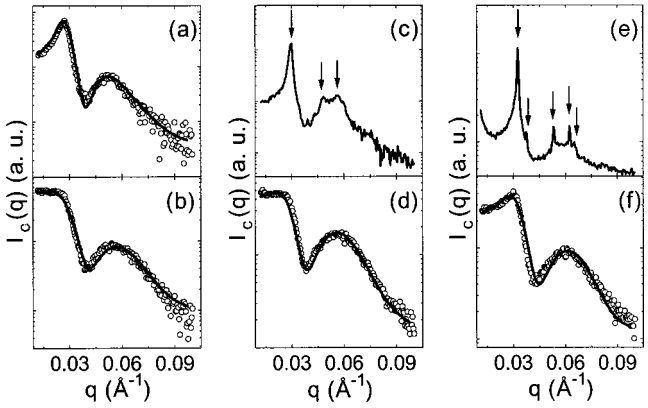

FIG. 3. Representative SAXS data with fits to models using structure factors for the hard sphere model. Profiles are shown for (a) 8 wt % gel, $T=25\,^{\circ}\mathrm{C}$; (b) 8 wt % gel, $T=70\,^{\circ}\mathrm{C}$; (c) 11 wt % gel, $T=25\,^{\circ}\mathrm{C}$ (the arrows indicate the positions of reflections associated with partial crystalline order); (d) 11 wt % gel, $T=70\,^{\circ}\mathrm{C}$; (e) 12 wt % gel, $T=25\,^{\circ}\mathrm{C}$ (the arrows indicate the positions of reflections for a face-centered-cubic structure); (f) 12 wt % gel, $T=70\,^{\circ}\mathrm{C}$.

Typical fits to SAXS intensity profiles using the hard sphere model are shown in Fig. 3. The corresponding parameters are listed in Table I. For the 8 wt % sample a weak structure factor maximum at $q^{*}=0.028\,\text{Å}^{-1}$ evident at 25 °C [Fig. 3(a)] disappears on heating to 70 °C. The scattering profile [Fig. 3(b)] then resembles that obtained for a dilute solution (2 wt %) where structure factor effects are absent. Figure 3 also shows the high-quality nature of the fits to the data using our model based on the hard sphere structure factor.

At higher polymer concentrations, the soft solid phase can be accessed. Figure 3(c) shows the scattering profile from this structure, which suggests partial crystalline order (higher order reflections are present in the SAXS profile). Neither the splitting of the second peak, nor the first maximum and overall shape of the scattering profile can be described by the liquid state model. In fact, the SAXS data in the soft solid region can be ascribed to a coexistence of liquid and solid phases, the profile in the soft solid being represented as a sum of that from liquid and solid phases as illustrated in Fig. 4.

TABLE I. Micellar dimensions from SAXS data. Included are the radius of gyration of the E block, R_g, and the radius of the hydrophobic core, R_s (both obtained from the form factor).

c (wt %)	T (°C)	R_g (Å)	R_s (Å)
8	25	34.0	40.5
	70	20.0	42.8
10	25	32.0	41.0
	70	21.1	42.9
11	36	30.5	43.0
	70	19.8	45.1
12	52	26.6	43.3
	70	20.0	44.0

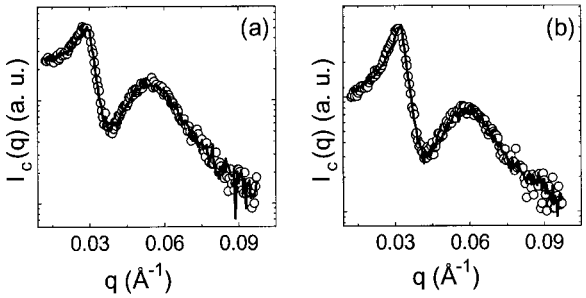

FIG. 4. SAXS data in the soft solid region (○) and summed profiles from fractional addition of SAXS profiles in solid and liquid phases (solid line) for $E_{87}B_{18}$. (a) At 47 °C for 11 wt % $E_{87}B_{18}$ the solid line corresponds to 10% and 90% contributions from SAXS profiles at 25 and 52 °C, respectively, (b) at 52 °C for 12 wt % $E_{87}B_{18}$ the solid line corresponds to 50% and 50% contribution from SAXS profiles at 36 and 62 °C, respectively.

On heating an 11 wt % solution, a transition to the liquid phase occurs near 40 °C. The SAXS profile in Fig. 3(d) shows that interparticle interactions in the liquid at 70 °C are very weak. SAXS patterns obtained from a 12 wt % sample are shown in Fig. 3(e) and Fig. 3(f). The low-temperature solid is characterized by a SAXS pattern from a face-centered-cubic crystal [the arrows in Fig. 3(c) indicate the positions of allowed reflections for the $Fm\bar{3}m$ space group]. At 70 °C, the profile in Fig. 3(f) is consistent with a liquid structure in which intermolecular interactions are still present as shown by the presence of a structure factor peak.

Figure 5 shows the volume fractions determined from the structure factor using the hard sphere model, superposed on the phase diagram determined from rheology (Fig. 1). The volume fractions in the liquid phase are below those for melting ($\phi_m=0.545$) or freezing ($\phi_f=0.494$) of hard spheres. The equilibrium phase is fluid at volume fractions lower than ϕ_f and crystalline at volume fractions higher than

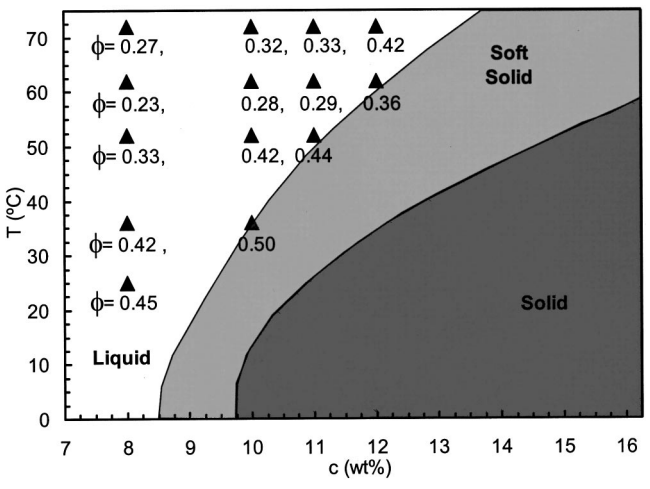

FIG. 5. Volume fractions determined from the hard sphere structure factor superposed on the gel diagram obtained from rheology (Fig. 1).

ϕ_m, with the two phases coexisting between these values. Interestingly, the hard sphere structure factor model could be applied even in the soft solid region: values for volume fractions obtained (data not shown) fall between these two volume fractions, again consistent with coexistence. Thus the soft solid in $E_{87}B_{18}$ appears not to be associated with a percolated network of micelles. These results differ from those obtained from small-angle neutron scattering/rheology studies of aqueous solutions of triblock $E_{13}P_{30}E_{13}$ [13,14] where the percolation line was crossed for solutions containing 5–50 % polymer [14]. A major difference in the phase diagram of this copolymer compared to $E_{87}B_{18}$ is the presence of a clouding transition at high temperatures in the former. This is consistent with the higher hydrophobic block content (48 wt % for $E_{13}P_{30}E_{13}$ versus 25 wt % for $E_{87}B_{18}$). This enhances the tendency for phase separation as the solvent quality for poly(oxyethylene) declines at high temperature. Phase separation results from a decrease in polymer-solvent contacts at the expense of polymer-polymer contacts, in other words there is an effective attraction between the copolymer chains. For more hydrophobic blocks, this attraction is enhanced. It thus appears that the aggregation of micelles upon increasing polymer concentration is nonuniversal, and depending on the copolymer composition (and molecular weight) the soft gel may either be a percolated micellar network or coexisting liquid and crystalline phases.

In summary, we have shown that the soft solid formed by a diblock copolymer in a selective solvent contains coexisting liquid micellar and crystalline solid phases. In contrast to previous reports for a related amphiphilic triblock copolymer [13,14], a percolation transition is not observed. The hard sphere approximation describes the intermicellar interactions well over the range of temperatures and concentrations accessed. It is hoped that our work on block copolymer micelles stimulates further studies into aggregation and crystallization phenomena in these model hard sphere systems.

This work was supported by EPSRC, UK (Grant Nos. GR/M51994 and GR/N22052). C.C. was supported by the EU-TMR network ''Complex Architectures in Diblock Copolymer-Based Polymer Systems.'' We thank Professor Jan Skov Pedersen and Professor Wilson Poon for helpful discussions.

[1] W. G. Hoover and F. H. Ree, J. Chem. Phys. **49**, 3609 (1968).
[2] P. N. Pusey and W. van Megen, Nature (London) **320**, 340 (1986).
[3] H. Watanabe, T. Kotaka, T. Hashimoto, M. Shibayama, and H. Kawai, J. Rheol. **26**, 153 (1982).
[4] K. Mortensen, W. Brown, and B. Nordén, Phys. Rev. Lett. **68**, 2340 (1992).
[5] G. A. McConnell, A. P. Gast, J. S. Huang, and S. D. Smith, Phys. Rev. Lett. **71**, 2102 (1993).
[6] I. W. Hamley, J. P. A. Fairclough, A. J. Ryan, C. Y. Ryu, T. P. Lodge, A. J. Gleeson, and J. S. Pedersen, Macromolecules **31**, 1188 (1998).
[7] S. Hvidt, E. B. Jørgensen, K. Schillén, and W. Brown, J. Phys. Chem. **98**, 12 320 (1994).
[8] I. W. Hamley, C. Daniel, W. Mingvanish, S.-M. Mai, C. Booth, L. Messe, and A. J. Ryan, Langmuir **16**, 2508 (2000).
[9] G. A. McConnell, E. K. Lin, A. P. Gast, J. S. Huang, M. Y. Lin, and S. D. Smith, Faraday Discuss. **98**, 121 (1994).
[10] M. Watzlawek, C. N. Likos, and H. Löwen, Phys. Rev. Lett. **82**, 5289 (1999).
[11] P. C. Hemmer, E. Velasco, L. Mederos, G. Navascués, and G. Stell, J. Chem. Phys. **114**, 2268 (2001).
[12] H. Li, G.-E. Yu, C. Price, C. Booth, E. Hecht, and H. Hoffmann, Macromolecules **30**, 1347 (1997).
[13] L. Lobry, N. Micali, F. Mallamace, C. Liao, and S.-H. Chen, Phys. Rev. E **60**, 7076 (1999).
[14] S.-H. Chen, C. Liao, E. Fratini, P. Baglioni, and F. Mallamace, Colloids Surf., A **183-185**, 95 (2001).
[15] I. W. Hamley, Philos. Trans. R. Soc. London, Ser. A **359**, 1017 (2001).
[16] I. W. Hamley, J. A. Pople, J. P. A. Fairclough, N. J. Terrill, A. J. Ryan, C. Booth, G.-E. Yu, O. Diat, K. Almdal, K. Mortensen, and M. Vigild, J. Chem. Phys. **108**, 6929 (1998).
[17] V. Castelletto, C. Caillet, J. Fundin, I. W. Hamley, and Z. Yang, J. Chem. Phys. (to be published).
[18] J. A. Pople, I. W. Hamley, J. P. A. Fairclough, A. J. Ryan, B. U. Komanschek, A. J. Gleeson, G.-E. Yu, and C. Booth, Macromolecules **30**, 5721 (1997).
[19] H. H. Winter and M. Mours, Adv. Polym. Sci. **134**, 165 (1997).
[20] B. Derrida, D. Stauffer, H. J. Herrmann, and J. Vannimenus, J. Phys. (France) Lett. **44**, L701 (1983).
[21] H. J. Herrmann, B. Derrida, and J. Vannimenus, Phys. Rev. B **30**, 4080 (1984).
[22] P. G. de Gennes, C. R. Acad. Sci. B **286**, 131 (1978).
[23] F. Mallamace, S.-H. Chen, Y. Liu, L. Lobry, and N. Micali, Physica A **266**, 123 (1999).
[24] J. S. Pedersen, J. Appl. Crystallogr. **27**, 595 (1994).
[25] J. S. Pedersen and M. C. Gerstenberg, Macromolecules **29**, 1363 (1996).
[26] N. W. Ashcroft and J. Lekner, Phys. Rev. **145**, 83 (1966).